Flow and Heat Transfer Analysis in Solar Chimney Power Plant with Sloped Roof

Gaci Farid[1], Bensouici Moumtez[2]

[1] Transport Engineering Department, Sciences of Technology Faculty, Frères Mentouri University, Constantine1, Algeria

[2]Electrotechnic Department, Sciences of Technology Faculty, Frères Mentouri University, Constantine1, Algeria

*Corresponding author; Email: fd.gaci@gmail.com

Article Info

Article history:

Received, 13/11/2023
Revised, 10/12/2023
Accepted, 12/12/2023

Keywords:

Solar chimney
insolation
turbulence
radiation
CFD

ABSTRACT

This paper presents a numerical study of natural convection in a solar chimney with a sloped roof designed for renewable energy production. Numerical analysis was carried out by using the Fluent 6.3.26 with a Reynolds-Averaged Navier-Stokes approach. Different turbulence models and Boussinesq approximation for buoyancy-driven flow are used. A parametric study on the performance power output of the solar chimney at various geometric parameters and different insolation levels was carried out to investigate the relationship between them. The numerical results obtained highlight the influence of these parameters.

I. Introduction

In the last decades, with the continuous fossil fuels depletion and the ecological environment's gradual deterioration, the vigorous development of renewable energy has become a basic economic necessity [1-5]. The most interesting topic in the renewable energy sector is that of solar energy converters. The solar chimney power plant (SCPP) seems to be an alternative for electrical power generation. The SCPP system relies on the greenhouse effect and stack effect to drive the turbine generator to produce electricity. Solar radiation penetrates the collector and heats the ambient air (greenhouse effect). The thermal energy emitted by the sun is captured by the collector heats the ambient air (greenhouse effect) which will flow towards the outlet of the collector, which is also the inlet of the chimney caused by the pushing force of Archimedes.

Compared with solar thermal systems and photovoltaic energy technology, the SCPP system boasts four distinct advantages for generating electricity through solar energy: low technical threshold, convenient maintenance, durable operation, and better environmental benefits. In the eighties, the first 50 kW prototype was in operation in Manzanares (Ciudad Real), working for more than 15,000 hours. Thanks to these tests, several projects are being carried out around the world, including a 40 MW plant in Ciudad Real and another 100 MW plant in Australia with chimneys of 750 and 1,000 meters respectively.

In recent years, many papers on chimney solar power generation systems have been published [6-10], including theoretical analysis and experimental research. The principle of this energy production system was developed by J. Schliach in his book "The Solar Chimney" [11].

This study uses numerical simulations to analyze two-dimensional turbulent airflow in a chimney plant driven by greenhouse and chimney effects. Particular attention is paid to the variation in the SCPP performance system under different parameters.

II. Problem Description and Numerical Details

The solar chimney geometry is illustrated in Figure 1. The chimney has a diameter of 10 m and stands 200 m in height. The sloped collector (θ=10°) has a diameter of 244 m and 5 m deep. There is a gap of 2 m between the transparent cover and the ground above the collector, so the height of the chimney outlet will increase by 2 m. These dimensional parameters apply to power plant design with only the underground soil as the heat storage system. The geometry is created and meshed using the Gambit software 2.4.6.

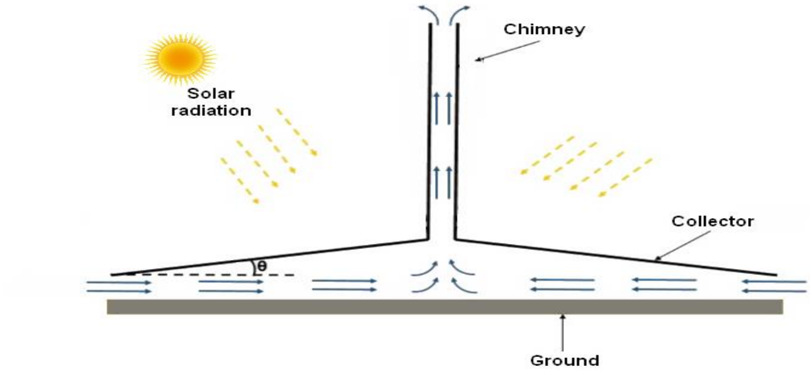

Figure 1. Geometric configuration of the problem

The axisymmetric steady turbulent flow of an incompressible fluid is governed by the continuity, momentum, and energy equations, written in conservative form.

$$\frac{\partial \bar{U}_i}{\partial x_i} = 0 \tag{1}$$

$$\frac{\partial}{\partial x_i}\left(\bar{U}_i \bar{U}_j\right) = -\frac{\partial \bar{P}_i}{\partial x_i} + \frac{\partial}{\partial x_j}\left[\mu \frac{\partial \bar{U}_i}{\partial x_i} - \rho \overline{u_i u_j}\right] \tag{2}$$

$$\frac{\partial T}{\partial x_i} + \frac{\partial}{\partial x_j}\left(T U_j\right) = \alpha \frac{\partial^2 T}{\partial^2 x_i^2} \tag{3}$$

Where T, α, $\bar{U}_i$, $\bar{P}$, μ, ρ *and* $-\overline{u_i u_j}$ represent the temperature, the thermal diffusivity, the average velocity component in the x_i direction, the average pressure, the dynamic viscosity, the density, and a component of the Reynolds stress tensor respectively.

There are various turbulent models used in the present work to compute the unknown Reynolds stresses, namely, the two equations k-ε standard, RNG k-ε and Realizable k-ε models, and the seven-equation Reynolds stress model.

We utilized Fluent software for the numerical solution of the governing equations, which include the Navier-Stokes equations for fluid flow and energy equations for heat transfer. The SIMPLE algorithm addressed pressure-velocity coupling, while a second-order upwind scheme ensured accurate discretization of convection terms within all transport equations. For more details on mathematical solving, please refer to Fluent's theory guide manual.

Among different radiation models, the discrete ordinates (DO) model stood out for its enhanced accuracy in simulating radiation energy transfer processes within the solar chimney. Furthermore, the DO model allows for the direct incorporation of discrete solar load data, making it a more suitable choice for our analysis. The most important condition is that the density change is not too large or the temperature difference is not too large. Fortunately, many natural convection problems in engineering can meet these conditions. A more theoretical expression is, β|(T-T0)|<<1, where β is the thermal expansion coefficient, T is the computational domain local temperature (or the temperature of each discrete unit), and To is the Boussinesq reference temperature. To avoid numerical oscillations and ensure convergence, we applied under-relaxation factors to the discretized equations. The convergence criterion is set at 10^{-5} for continuity and momentum equations, whereas for the energy equation, it is set at 10^{-7}. The boundary conditions considered in the present simulations: The ground of the heat collector is defined as a boundary of constant heat flux and for different radiation intensities, here is the absorbed solar energy. The wall of the chimney and the top of the collector are both defined as mixed boundaries, which means there is heat loss here. All the side faces of energy storage layers are considered to be adiabatic.

Boundary conditions considered in present simulations are: The ground is defined as a boundary of constant heat flux and for different radiation intensities. The collector is defined as a mixed boundary, which means there is heat loss here. The chimney wall is considered adiabatic

III. Results and Discussion

III.1. Grid Independence Study

Using the Gambit software 2.4.6, the mesh adopted in this investigation is quadrilateral uniform, figure 2 (a). Grid-independence tests were carried out. Satisfactory numbers of cells were found to vary between 860 and 1 35000. Figure 2(b) shows a velocity magnitude profile obtained using M_1 = 8606, M_2 = 33552, and M_3 = 135060 nodes at the collector center distance. In this case, the grid M_2 is selected.

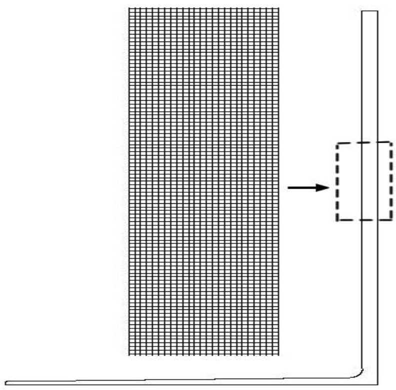

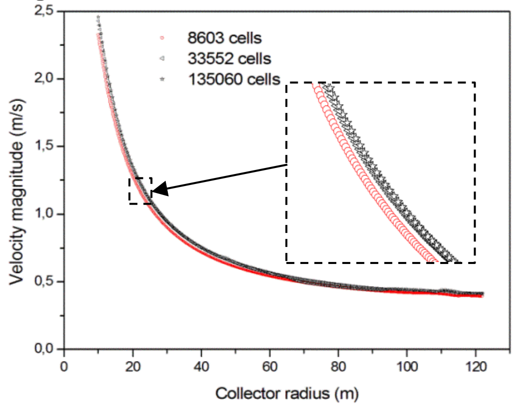

(a) (b)

Figure 2. Considered domain meshing (a) and velocity magnitude profile at the collector center (b)

III.2. Validation

The validity of the numerical simulation procedure was confirmed by comparing the dimensionless velocity profile versus the dimensionless chimney radius with the results obtained by Maia et al. (2009) [10]. While minor discrepancies exist compared to Maia et al.'s data (Figure 3), the overall agreement between our results remains satisfactory.

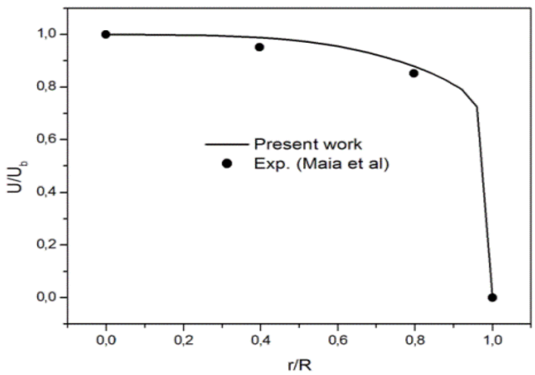

Figure 3. Dimensionless velocity profile0

III.3. Choice of Turbulence Model

There are two main considerations in choosing a turbulence model: computational cost and applicable field. The more accurate the turbulence model, the higher the computational cost. We need to choose the least-cost turbulence model that can meet our computational requirements based on our application area.

To test the effect of the turbulence model, the Reynolds average method (RANS: Reynolds Averaged Navier-Stokes) was used which is widely used in engineering and is a large family of turbulence models, which includes many sub-models. The RANS method expresses all physical quantities in a turbulent flow as a function of time and space and decomposes them into the superposition of time-averaged and fluctuating terms. From this family, we employed four turbulence models: three two-equation models (standard k-ε, RNG k-ε, and k-ε realizable) and one seven-equation Reynolds Stress Model (RSM). This comparison aimed to identify the most suitable model for accurately predicting the flow characteristics and guiding further analysis.

Figure 4 shows dimensionless velocity profiles at the chimney outlet for different turbulence models. Compared to the experimental data, the realizable k-ε model result is in good agreement and more satisfying than the other models.

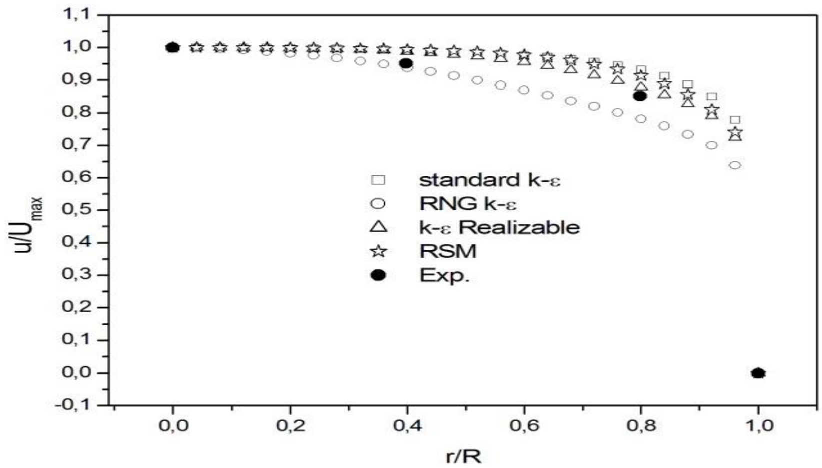

Figure 4. Dimensionless velocity profiles for different turbulence models

For understanding and simulating turbulent flows, turbulent kinetic energy (k), a measure of the average kinetic energy of turbulent eddies, is one of the most essential physical quantities. The turbulent diffusion is an important index to measure the development or decline of the turbulent flow and it can be estimated by the turbulence intensity and the average velocity. Figure 5 shows turbulence intensity from one model to another. The airflow recirculation zone near the outer wall of the chimney generally presents a dead mixing zone. This physical characteristic is best represented by the k-ε realizable model since hot air flows towards the central area of the heat sink during the buoyancy process, coupled with the enormous suction force generated by the stack effect, a strong updraft will be generated in the chimney creating a zone of turbulence at the entrance to the chimney tower near the outer wall.

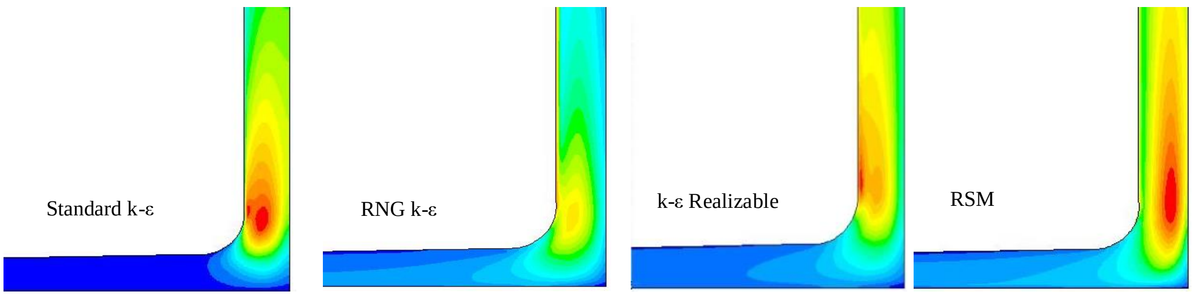

Figure 5. Turbulent Kinetic Energy contours for different turbulence models

As observed in Figure 6, the thermal field distribution under solar radiation of 400 W/^{m2} shows that the air temperature in the middle of the chimney initially decreases and remains relatively constant. This decrease in thermal energy relative to gravitational potential energy, as evidenced by the temperature profile, weakens the buoyancy effect of the air inside the chimney with increasing height.

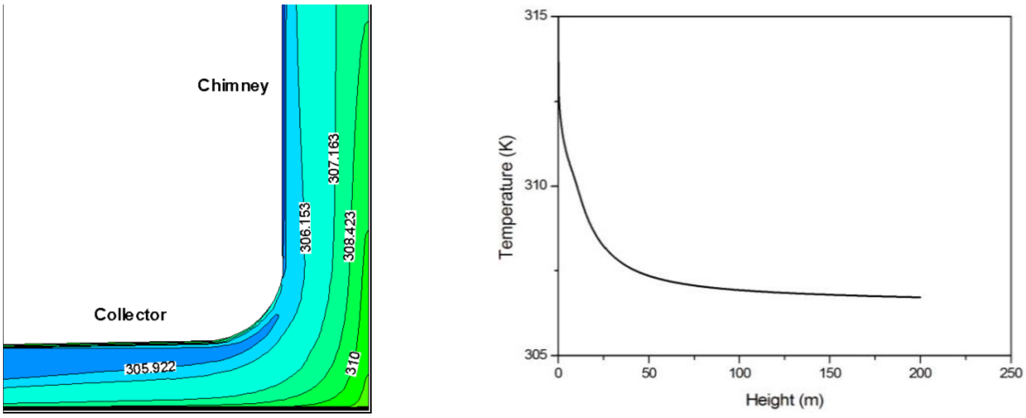

Figure 6. Chimney tower temperature evolution

III.4. Effect of Height Chimney Tower

Figure 7 shows the impact of increasing chimney height on the air velocity. The linear trend of the curve reveals a direct relationship, where a taller chimney leads to a higher mass flow of hot air inside due to an enhanced buoyancy effect with greater height difference.

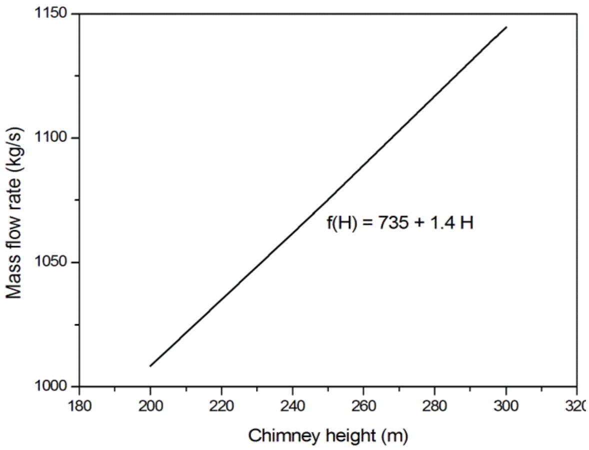

Figure 7. Mass flow rate evolution.

The relationship between the mass flow rate generated by the chimney effect and the stack height is described by a linear variation, which can be expressed as:

$$f(\mathrm{H}) = 1.4\ \mathrm{H} + 735 \qquad (4)$$

III.5. Effect of Solar Radiation

Since the SCPP can operate all day under variable solar radiation intensity G (400W/m^2, 800W/m^2, and 1000W/m^2), figure 8 illustrates the solar radiation effect on chimney outlet velocity generated to drive the turbine. We note that the evolution of the air velocity magnitude exit from the chimney represents an exponential function increasing with increasing solar radiation, figure 8(b). However, with decreasing chimney height, the velocity decreases and moves away from the chimney entrance, figure 8(a), or even from the location of the turbine.

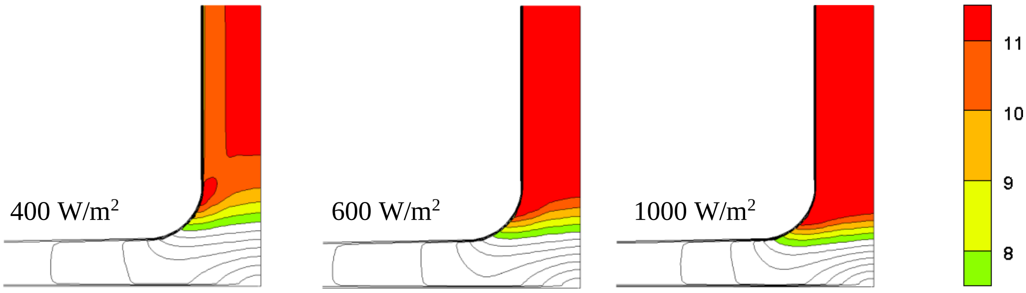

(a)

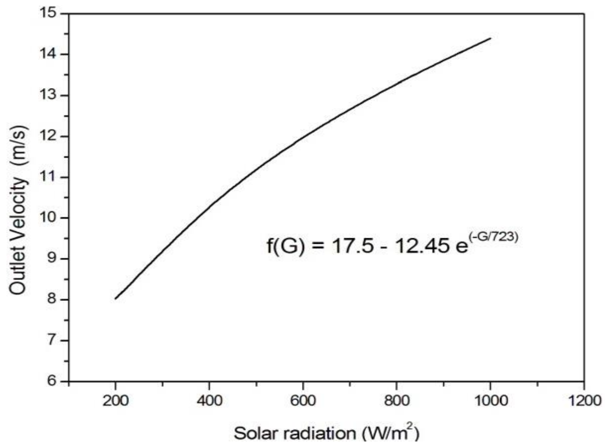

(b)

Figure 8. Contours of velocity magnitude (a) and profile solar radiation effect on outlet velocity (b)

IV. CONCLUSION

A two-dimensional turbulent airflow numerical analysis in a solar chimney under natural convection action has been presented. To understand the airflow within the solar chimney, we employed a numerical simulation based on fundamental equations governing mass, energy, and momentum conservation. In addition, we factored in the transport of turbulent properties. To ensure the accuracy of our model, we meticulously compared its results with data gathered by Maia et al. By varying parameters like chimney height and solar intensity, we were able to assess their impact on the chimney's overall performance.

Our result reveals a remarkable synergy between chimney height, solar radiation, and airspeed, the fuel for turbine rotation and electricity generation. As the chimney stretches skyward or solar radiation increases, the pressure difference across its length amplifies, creating a powerful draft that pulls air through its core. This surge in airflow directly translates to enhanced chimney power, driving increased turbine spin and ultimately, a richer harvest of electricity.

References

[1] Bahous N., Bentiallah D., Kalloum S., Bentiallah A. Amelioration of the Performance of Glass Solar Still Using Different Absorbers in Adrar. Algerian Journal of Renewable Energy and Sustainable Development, 2020, 2:137 — 150.

[2] Bencherif L., Bousskaia T., Benhammou M. Effect of the Double Glazing on the performance of an Air Solar Collector. Algerian Journal of Renewable Energy and Sustainable Development, 2020, 2: 42 — 50.

[3] Ghaitaoui T., Laribi S., Arama F.Z., Ben moussa F., Ghaitaoui E. A., Halali Y., Arbaoui I. Study and Simulation of Self-supply of a Building by Photovoltaic Energy. Algerian Journal of Renewable Energy and Sustainable Development, 2023, 1:70 — 78.

[4] Benabdelkrim B., Benatillah A., Ghaitaoui T., Hammaoui K. Experimental Analysis of a Photovoltaic Power Plant in a Desert Environment– Adrar area –. Algerian Journal of Renewable Energy and Sustainable Development, 2023, 3:85 — 96.

[5] Guentri H., Benasla M., Ezaeri K. The impact of Naama's 12 MW Solar Project on the Algerian Southwestern Electricity. Algerian Journal of Renewable Energy and Sustainable Development, 2020, 2:105 — 113.

[6] Pasumarthi N., Sherif, S A. Experimental and theoretical performance of a demonstration solar chimney model -Part Ⅰ:Mathematical model development. Int. J. of Energy Research, 1998, 22:277 — 288.

[7] Pasumarthi N., Sherif S A. Experimental and theoretical performance of a demonstration solar chimney model -Part Ⅱ: Experimental and theoretical results and economic analysis. Int. J. of Energy Research, 1998, 22:443— 461.

[8] Lodhi M A K. Application of helio-aero-gravity concept in producing energy and suppressing pollution. Energy Conversion & Management, 1999, 40:407 — 421.

[9] Dai Y., Huang H., Wang R. Research on the application of solar thermal wind power generation technology in Ningxia. Journal of Solar Energy Sinica, 2003.24(3):408-412.

[10] Yang J., Li Jin,. Xiao B. New technology of solar chimney power generation. Journal of Solar Energy, 2003, 24 (4): 565 — 569.

[11] Schlaich J. The solar chimney: electricity from the sun. Stuttgart: Axel Menges publisher; 1995.

[12] Gupta MK., Kaushik SC. Exergetic performance evaluation and parametric studies of the solar air heater. Energy 2008; 33:1691–702.

[13] Petela R. Thermodynamic study of a simplified model of the solar chimney power plant. Solar Energy 2009; 83:94–107.

[14] Koonsrisuk A., Lorente S., Bejan A. Constructal solar chimney configuration. Int J Heat Mass Transfer 2010; 53(1–3):327–33.

[15] Maia C.B., Ferreira A.G., Valle R.M. and Cortez M.F.B. Analysis of the Airflow in a Prototype of a Solar Chimney Dryer. Heat Transfer Engineering, Vol. 30, N°5, pp. 393 – 399, 2009.

[16] Patankar S.V. Numerical Heat Transfer and Fluid Flow, Hemisphere, New York, 1980.

[17] Al-Kayiem H.H., Sreejaya K.V., Gilani S. Mathematical analysis of the influence of the chimney height and collector area on the performance of a rooftop solar chimney. Energy Build. 68, pp. 305–311, 2014.

[18] Bassiouny R., Koura NSA. An analytical and numerical study of solar chimney use for room natural ventilation. Energy Buildings 2008; 40:865–73.

[19] MA dos S. Bernardes, Voß A., Weinrebe G. Thermal and technical analyses of solar chimneys. Sol. Energy 2003; 75:511–24.

[20] M.A dos S. Bernardes, Valle R., Cortez M.F.B. Numerical Analysis of Natural Laminar Convection in a Radial Solar Heater. International Journal of Thermal Sciences, Vol. 38, N°1, pp. 42 - 50, 1999.